XIX ANIDIS Conference, Seismic Engineering in Italy

Preliminary validation of an innovative stress sensor for the Structural Health Monitoring of masonry buildings

Alessia Monaco[a*], Gabriele Bertagnoli[b], Lidia La Mendola[c], Maria Concetta Oddo[c], Agatino Pennisi[d]

a DAD – Politecnico di Torino – V.le Mattioli, 39 – 10125 Torino, Italy
b DISEG – Politecnico di Torino – C.so Duca degli Abruzzi, 24 – 10129 Torino, Italy
c DI – Università di Palermo – Viale delle Scienze, Ed. 8 – 90128 Palermo, Italy
d STMicroelectronics – Stradale Primosole, 50 – 95121 Catania, Italy

Abstract

Structural Health Monitoring (SHM) of existing masonry constructions is a challenging topic widely studied by the scientific community. In this paper, the use of a low-cost Capacitive Stress Sensors (CSSs) is investigated as an effective tool for the detection of the compression state level in mortar joints of masonry structures. The study is conducted by means of Finite Element (FE) simulations aimed at reproducing the mechanical response of a prototype of innovative CSS, recently patented, subjected to compression forces typical of masonry buildings under serviceability conditions. The constitutive behaviour of the sensor is validated against the results of a pilot laboratory test on a mortar cylindrical specimen endowed with CSSs and LVDTs and then subjected to cyclic uniaxial compression. The FE model is built in order to simulate the capacitive sensor embedded within the mortar material; therefore, a correlation analysis is performed by comparing the numerical stress-strain output of the sensor and the experimental results. The validation procedure shows that the numerical results are in good agreement with the records obtained by the LVDTs. Moreover, the FE model is used for developing a parametric analysis aimed at highlighting the effects of mortar stiffness and strength on the efficacy of the SHM performed by the CSSs and the optimal serviceability configurations are accordingly identified.

Keywords: Structural health monitoring; capacitive stress sensors; numerical modelling; experimental tests; axially loaded cylinders.

* Corresponding author. Tel.: +39 011 090 4881; fax: +39 011 090 4881.
 E-mail address: alessia.monaco@polito.it

1. Introduction

The Structural Health Monitoring (SHM) of constructions is a challenging topic studied by the scientific community for decades. Today, the increasing evolution of sophisticated smart sensing technologies has inspired a growing interest in the real-time monitoring of the structural performance of both new and existing buildings and infrastructures. As a matter of fact, catastrophic events or even only the effects of the natural ageing of materials have highlighted the importance of detecting those structural changes that could be critical for the safety of the construction and the preservation of its serviceability state (Sohn et al. 2003, Boller et al. 2009, Balageas et al. 2010). Therefore, continuous monitoring of the main structural parameters helps detect the incoming critical states or damage with respect to proper target levels.

In this context, the present research focuses on the use of Capacitive Stress Sensors (CSSs) as an effective tool for performing the SHM of masonry buildings. In particular, innovative CSSs, recently patented (Bertagnoli 2016, Abbasi et al. 2017, Pappalardo et al. 2019), are adopted for the detection of the compression state level in the bed joints of masonry panels made of resisting blocks and mortar layers. The authors have already conducted some previous experimental studies to compare the efficacy of CSSs and piezoelectric ceramic sensors embedded in the mortar joints of masonry panels made of calcarenite stone and solid clay bricks (La Mendola et al. 2021). Conversely, this study is developed through Finite Element (FE) analyses focused on the simulation of the mechanical response of CSSs embedded within a volume of mortar and subjected to compression forces. In particular, the behaviour of the sensor is validated against the results of a pilot laboratory test on a cylindrical specimen subjected to cyclic uniaxial compression. During the casting, prototypes of the CSSs were introduced within the mortar cylinder; the sample was tested under compression using a universal testing machine with displacement control and LVDTs were placed for monitoring the local displacement and obtaining the stress-strain constitutive curve of the mortar specimen. The FE model is built to simulate the capacitive sensor embedded within the mortar material; therefore, a correlation analysis is performed by comparing the numerical stress-strain output of the sensor and the experimental results. The validation procedure shows that the numerical results are in good agreement with records obtained by LVDTs. Moreover, the FE model is used for developing a parametric analysis to highlight the effects of mortar stiffness and strength on the efficacy of the SHM performed by the CSSs. The optimal serviceability configurations are accordingly identified with reference to two different geometries of the CSS. In this way, the pilot laboratory test and its FE modelling can be used to design a future extensive experimental campaign for the calibration of the CSS prototypes, also providing relevant input for the successive industrialisation of this low-cost device for SHM.

The paper is organised into the following sections: the geometrical and mechanical features of the CSS and its modelling are presented in section 2; section 3 reports the correlation analysis between experimental and FE outcomes; in section 4, the numerical parametric analysis is developed for the assessment of the effects of the mortar features and the CSS geometry on the effectiveness of the monitoring system; finally, section 5 reports the main conclusions.

2. Capacity sensor architecture and modelling

The CSS prototype architecture derives from a deep experience previously developed on strain force sensors for SHM. In particular, the first sensors developed between 2012 and 2015 were based on the piezoresistive effect of Complementary Metal Oxide Semiconductor (CMOS) transistors on a silicon die. The size of those sensors was very small and the first studies had shown the relevant effect of the sensor dimensions on the monitoring of stresses in large structures. As a consequence, further studies were devoted to the development of a device endowed with a big sensing area directly faced with the surrounding material, such as mortar or concrete. These new studies led to a novel patented solution which is that considered in this paper (Pappalardo et al. 2019).

The CSS architecture is shown in Fig. 1: it is constituted by two parallel thin plates that make a capacitor with Kapton as the dielectric layer. More in detail, the architecture of the CSS is characterised by two external discs of copper with diameter 40 mm and thickness 35 μm; then, two layers of FR4 are collocated, with the same diameter of the outer copper disc and thickness equal to 0.8 mm. The dielectric layer of Kapton has a thickness of 25 μm and it is covered on the top and the bottom by two internal layers of copper in which two gaps are created: the gap on the top is equal to 0.5 mm while that on the bottom is 1 mm. The structure is completed by a tin welding of about 0.2 mm.

The capacitance of the sensor is calculated as:

$$C = \frac{\varepsilon_0 \cdot \varepsilon_r \cdot A}{d} \tag{1}$$

In Eq. (1), ε_0 is the vacuum dielectric constant $\varepsilon_0 = 8.8542 \cdot 10^{-3}$ pF/mm and ε_r is the Kapton dielectric constant $\varepsilon_r = 3.4$ while A and d are respectively the area of the electrodes and the gap between them. The area of the capacitor is $A = 346.36$ mm^2 and the opening corresponds to the thickness of the Kapton.

The architecture of the system is modelled through the FE method taking advantage of its symmetry in order to generate an axisymmetric model with the finite element software Abaqus (Abaqus/CAE 2020). The finite elements used for all material layers are linear quadrilateral elements of type CAX4R, with an average mesh size of 25×75 μm for Kapton and copper and 100×75 μm for the FR4.

The constitutive behaviour assumed for the modelling of the copper layers is linearly elastic and isotropic, with elastic modulus $E_{copper} = 128$ GPa and Poisson's coefficient $\nu_{copper} = 0.36$. Also the Kapton is modelled by adopting a linear elastic behaviour, with $E_{Kapton} = 2.5$ GPa and $\nu_{Kapton} = 0.34$. Conversely, the constitutive model assumed for the FR4 layers is a transversally isotropic linear elastic behaviour with in-plane elastic modulus $E_{FR4,p} = 20$ GPa and transversal elastic modulus $E_{FR4,t} = 2$ GPa. The primary Poisson's ratio is 0.2.

1. Copper: D=40mm; s= 35μm 2. FR4: D=40mm; s=0.8 mm 3. Kapton: D=40mm; s=25μm
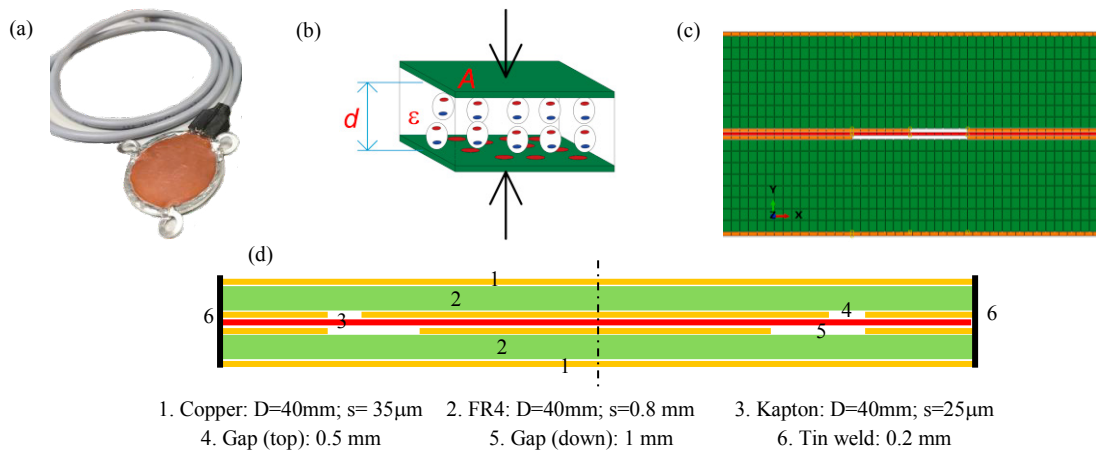4. Gap (top): 0.5 mm 5. Gap (down): 1 mm 6. Tin weld: 0.2 mm

Fig. 1. CSS architecture: (a) global view; (b) electrical scheme; (c) detail of the mesh; (d) dimensions.

3. Numerical vs experimental correlation analysis

3.1. Description of the experimental tests

The numerical modelling of the CSS behaviour is validated against the results of a cyclic uniaxial compression test conducted on a pilot cylindrical mortar specimen endowed with both CSSs inside and LVDTs on the external surface. The test has been conducted at the Laboratory of Materials and Structures of University of Palermo. The diameter of the tested sample is 160 mm and the height 340 mm. Three LVDTs are placed at 120° according to the scheme reported in Fig. 2; similarly, three CSSs are placed inside the specimen, in correspondence to the three external LVDTs, in the mid-section plane of the cylinder. A universal testing machine is used for applying a cyclic loading history able to induce in the specimen a uniform uniaxial compression. The loading history is reported in Fig. 3: the load is applied in displacement control until displacement values that correspond to the loading force in the intervals reported in the figure. In detail, in the first loading phase, three loading/unloading cycles between 0-18 kN are applied; in the second phase, the loading/unloading cycles are in the range 0-35 kN, while in the third phase, the loading/unloading interval is 0-55 kN. The maximum loading force is set in order to achieve about the 40% of the mortar compressive strength, which is equal to 6.3 MPa. The elastic modulus of the mortar is 6 GPa. Both compressive strength and elastic modulus

are obtained as the average values of the results of classical tests for the mechanical characterisation of nine specimens of mortar prisms, which are not reported here for brevity.

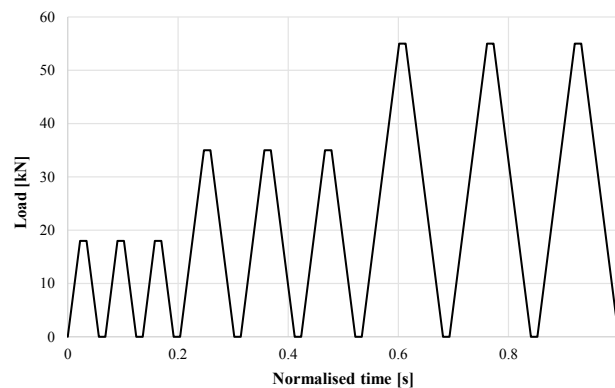Fig. 2. Instrumentation of the pilot mortar specimen and test setup.

Fig. 3. Cyclic loading history.

3.2. FE model

For the modelling of the tested cylinder, the CSS has the features already described in Section 2. Conversely, as regards the mortar, linear quadrilateral and triangular elements are used, with variable mesh size, which is more refined in the area next to the CSS location and greater in the other area of the model. Elements of dimension 0.5×0.4 mm are adopted next to the capacity sensor, while a mesh size of about 4×4 mm is used in the area next to the applied load and the support. The constitutive model adopted for the mortar material is non-linear. In detail, the Concrete Damaged Plasticity model is used to simulate its inelastic compressive and tensile behaviour. The compressive stress-strain relationship is deduced from the experimental characterisation of nine mortar prims by applying the analytical formulation by Saenz (1964) for the stress-strain response of unconfined concrete. Conversely, the tensile behaviour is modelled in terms of tensile stress-crack opening according to CEB-FIB Model Code 2010 (CEB-FIB 2010).

Appropriate interaction properties are finally modelled for the simulation of the contact between the sensor components and between the CSS and the surrounding mortar. More in detail, a frictional behaviour with a friction coefficient equal to 0.5 is used for the contact between the external copper plates and the mortar material; perfect bond is modelled instead for the copper-to-FR4 interfaces using a kinematic constraint which enforces all connected nodes to have the same degrees of freedom. Finally, a frictionless interaction property is applied to the copper-to-Kapton interface. All normal contacts in compression are assumed rigid. The scheme of the set interfacial behaviour is reported in Fig. 4.
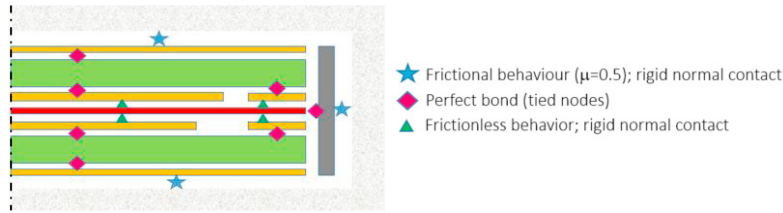
Fig. 4. Scheme of the modelled interface properties.

3.3. Correlation analysis

The correlation analysis is firstly conducted by validating the FE results against the experimental outcomes given by the LVDTs measurements. Fig. 5 shows the comparison between experimental and FE strain percentages; the abscissa of the graph reports the execution time of the laboratory test and the numerical analysis time normalised with respect to a unitary time interval of 0-1 seconds. The experimental measurements obtained from the LVDTs show that the laboratory test was affected by an eccentricity effect which is not considered in the FE model, where the applied load is perfectly uniaxial. Nevertheless, the average LVDT measurements (average between LVDT1, LVDT2 and LVDT3 records) and the FE strain values are compared and show quite good agreement in the first loading cycles (0-18 kN) and an average numerical underestimation of the measured strains of about 20% in the loading range 0-35 kN and 25% in the loading range 0-55 kN.
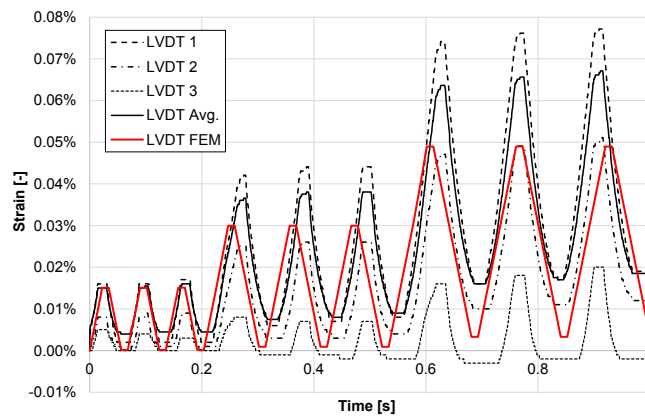

Fig. 5. Experimental vs numerical strain measurements.

The CSS measurements in laboratory are obtained in terms of capacitance variation, which occurs when the initial distance between the electrodes changes with the alternation of the loading and unloading cycles to which the mortar cylinder is subjected. Therefore, exploiting Eq. (1), for every variation of the capacitance C, the variation of the distance d can be calculated and, consequently, the strain assessment can be performed from the CSS records. Each sensor, then, needs a calibration procedure aimed at aligning its strain assessment with the strain measurements given by the LVDTs. In particular, several best-fitting scaling coefficients k_i can be calculated for the calibration of each CSS. Such coefficients are reported in Table 1 for each sensor and each loading phase. Moreover, with the aim of conducting a linear and constant scaling of the CSS measurements all over the cyclic test, three main scaling factors can be assessed, each one for the corresponding sensor: $k_1 = 210$, for the CSS named n-T6 which is associated to LVDT1; $k_2 = 650$, for the CSS named n-T2 which is associated to LVDT2; $k_3 = 1100$, for the CSS named n-T4 which is associated to LVDT3. These coefficients are used to reduce the strain measurements of the sensors and align the values to those measured by the LVDTs. Fig. 6 shows the strain values obtained by the CSSs scaled to the LVDT measurements for every CSS and every associated LVDT. In the same graph, the average CSS and LVDT measurements are reported for comparison (see the red solid and dashed lines).

Table 1. Scaling coefficients k_i for the CSS calibration.

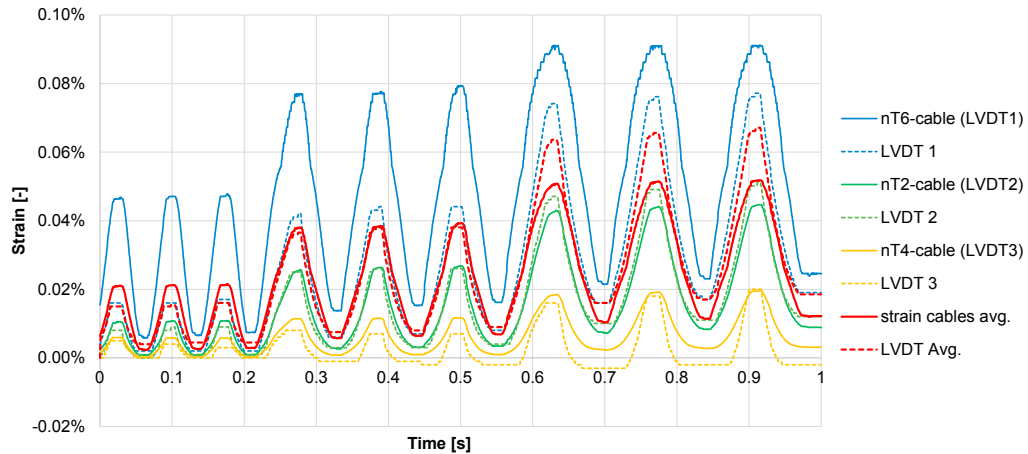|	0-18 kN	0-35 kN	0-55 kN
k_1	600	390	258
k_2	820	650	570
k_3	1100	1100	1100

Fig. 6. Strain values obtained by the CSSs scaled to the LVDT measurements.

Therefore, the strain values of the CSSs scaled by means of the correlation coefficients k_i are then compared with the FE strain values in the capacity sensor components. In particular, Fig. 7 reports the elastic strain in the direction of the applied load (E22) of the dielectric layer of Kapton, the external layer of copper plate and the FR4 strip. For completeness, also the strains in the mortar, corresponding to the LVDT position, are reported (LVDT FEM). These numerical strain values are compared with the average strains obtained by the CSS. As expected, it can be observed that the average strains of the sensors are closest to those recorded in the mortar in the proximity of the LVDT location, due to the scaling process adopted for the alignment of the strain records. Conversely, the model shows higher values of strains in the constituent materials of the capacity sensor and this phenomenon is also emphasised by the fact that the FE model is not affected by any imperfection present in laboratory or due to the manufacturing process of the capacity sensor.
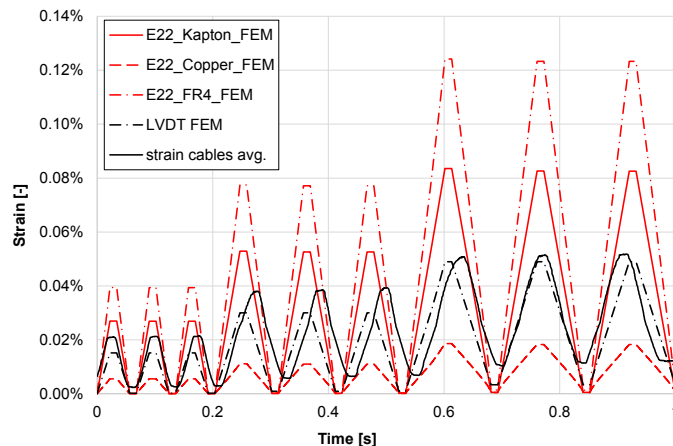

Fig. 7. Comparison between the average CSS strain measurements and the FE strain values in the capacity sensor's components.

4. Finite element parametric simulations

A parametric analysis is conducted in order to investigate, firstly, the influence of the mechanical features of the mortar on the effectiveness of the monitoring system. Successively, also the geometry of the CSS will be analysed.

In particular, an axisymmetric model is generated, in which a CSS is enclosed within a cylinder of mortar in the mid-section plane and with its central axis corresponding to the axis of symmetry of the cylinder. Two materials are investigated, namely, a low-stiffness and a medium-strength mortar. The low-stiffness mortar has a compressive strength of 8 MPa and an elastic modulus of 0.8 GPa. The simulation is developed, in this case, by applying a uniform uniaxial compression to the cylinder equal to 5.4 MPa (about 70% of the compressive strength). Conversely, the medium-strength mortar has a compressive strength of 14 MPa and an elastic modulus of 6.4 GPa and the specimen is loaded with a pressure equal to 10 MPa (about 70% of the compressive strength). The geometry of the sensor assumed in these analyses is called geometry type A and corresponds to that described in the previous sections of the paper (i.e. the effective gap in the copper inner plate is equal to 1 mm). Fig. 8 shows the comparison between the two numerical results: on the left, the low-stiffness mortar outcomes are reported, while on the right, those of the medium-strength mortar specimen. More in detail, the stresses in the Kapton layer are depicted together with the stresses in the surrounding mortar material, assessed at a distance of 1.5, 3.5 and 10 mm from the CSS location. Also the colour map of the strains is reported. It can be observed how the lower the stiffness of the material, the higher the cracking effect on the mortar close to the right end of the CSS, where the contact between sensor and mortar has to develop around a really small area, next to the tip of the sensor. Conversely, this effect is reduced when the stiffness of the mortar is much higher (one order of magnitude), and also the noise in the distribution of the stresses along the Kapton layer is limited in the second case. The noise effects are evaluated also considering a different geometry of the sensor, named geometry type B, in which the effective gap of the copper inner plate is greater, equal to 5 mm. From Fig. 9, it is possible to observe how an increased gap size induces a relevant noise even in the proximity of the sensing area, and this confirms that the CSS functioning benefits from larger sensing areas, which are therefore recommended.
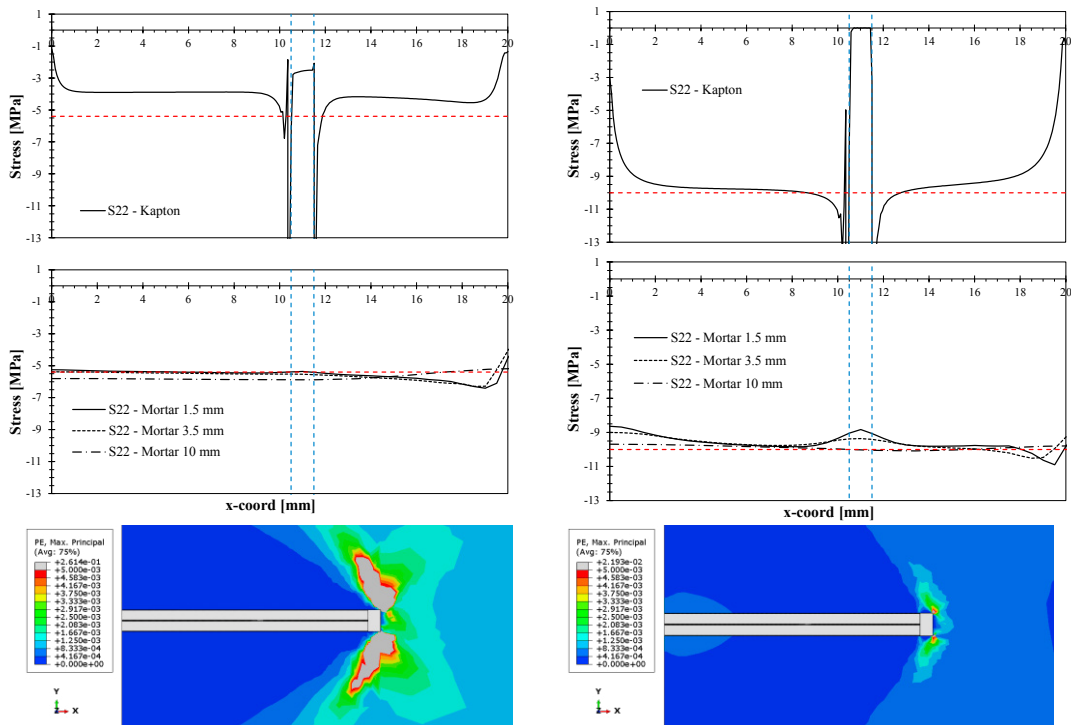

Fig. 8. Geometry type A (gap 1mm): low stiffness-mortar (left); medium-strength mortar (right).
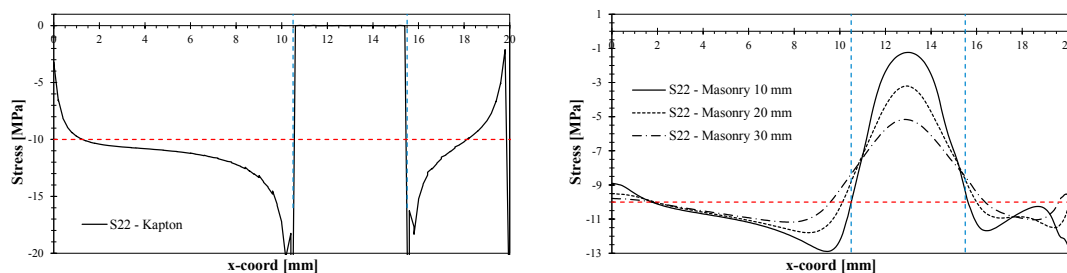
Fig. 9. Medium-strength mortar specimen with sensor of geometry type B (gap 5mm).

5. Conclusions

In this paper, Capacity Stress Sensors have been studied for the structural monitoring of masonry constructions. The study has been developed using the FE method for the validation of the sensor behaviour in the measuring of compressive strains in a mortar cylinder. A pilot cyclic uniaxial compression test has been performed in laboratory, adopting three different loading ranges for a specimen endowed with both internal CSSs and external transducers LVDTs at 120°. The variation of capacitance of the CSSs has been measured and scaling coefficients have been individuated for the calibration of the CSS, in order to align the strains estimated from the capacitance records with those measured by the LVDTs. A numerical FE model has been generated for the validation of the sensors. The model allows finding that the strain values obtained in the dielectric Kapton layer are higher than those measured in the mortar cylinder in the section where the LVDTs are applied. Nevertheless, it has to be remarked that the FE model is not affected by those imperfections typical of an experimental test and present in the manufacturing process of these sensor prototypes. Finally, a parametric analysis is conducted to evaluate the influence of the mortar mechanical properties and the sensor geometry on the effectiveness of the CSS, finding that the sensors benefit from larger sensing areas and that the higher the stiffness of the mortar, the lower the noise areas in the proximity of the CSS location. The results of this pilot study are preparatory for a future extensive experimental campaign for the calibration of the CSS prototypes and useful for the industrialisation process of these low-cost devices for the SHM.

Acknowledgements

References

Abaqus/CAE 2020, Dassault Systèmes Simulia Corp., Johnston, RI, USA.

Abbasi, M., Bertagnoli, G., Caltabiano, D., Guidetti, E. (inventors). ST Microelectronics s.r.l. (Assignee). Stress sensor for monitoring the health state of fabricated structures such as constructions, buildings, infrastructures and the like, Patent No. EP 3 392 637 B1, 2017.

Balageas, D., Fritzen, C. P., & Güemes, A. (Eds.). 2010. Structural health monitoring (Vol. 90). John Wiley & Sons.

Bertagnoli, G. (inventor). Safecertifiedstructures Tecnologia (Assignee). Method and investigation device for measuring stresses in an agglomerate structure, Patent No. WO2017/178985 A1, 2016.

Bertagnoli, G., Ciccone, E., Monaco, A., La Mendola, L. 2022. Finite element modelling of a Capacitive Stress Sensor. 7th World Multidisciplinary Civil Engineering-Architecture-Urban Planning Symposium WMCAUS 2022, 5-9 Sept. 2022, Prague (Czech Republic).

Boller, C., Chang, F. K., & Fujino, Y. (Eds.). 2009. Encyclopedia of structural health monitoring (Vol. 2960). New York: Wiley.

CEB-FIB 2010, fib Model Code 2010. Comité Euro-International du Béton.

La Mendola, L., Oddo, M. C., Papia, M., Pappalardo, F., Pennisi, A., Bertagnoli, G., Di Trapani, F., Monaco, A., Parisi, F., Barile, S. 2021. Performance of two innovative stress sensors embedded in mortar joints of new masonry elements. Constr Build Mater, 297, 123764.

Pappalardo, F., Pennisi, A., Guidetti, E., Doriani, A. (inventors). Capacitive pressure sensor for monitoring construction structures, particularly made of concrete, Patent n. US2019/0011320 A1, 2019.

Saenz, L. P. 1964. Discussion of "Equation for the stress-strain curve of concrete," by Desayi & Krishnan. ACI Struct. Journal 61 (9):1229-1235.

Sohn, H., Farrar, C. R., Hemez, F. M., Shunk, D. D., Stinemates, D. W., Nadler, B. R., Czarnecki, J. J. 2003. A review of structural health monitoring literature: 1996–2001. Los Alamos National Laboratory, USA, 1.